

Quantification of Wake Vortices Around Tandem Piers on Rigid Bed Channel



L. N. Pasupuleti, P. V. Timbadiya, and P. L. Patel

Abstract The current study focused on the strengths of wake vortices diffuse from pier boundary through velocity power spectra at 5, 30, and 50% of flow depth for piers arranged in tandem configuration. The experimental investigations were carried using the instantaneous 3D velocity measurements, undertaken using 16 MHz micro down looking Acoustic Doppler Velocimeter (ADV) at different grids along with flow depth for single and tandem piers. The measurements around two piers having the same diameter (separated by longitudinal distance $2d$) ($d = 8.8$ cm) at different levels of flow depth have been carried out and made comparison with a single pier on rigid bed condition under same flow conditions. The analysis of velocity power spectra is used to identify the inference of wake vortices of one pier over others in tandem arrangement vis-à-vis a single pier. The results reveal that the strengths of wake vortices are decreased by 2.5 times at level 5% of flow depth for the front tandem pier than that of a single pier. These strengths are increased while moving away from the bed in both cases. Further, the Strouhal number (St) of single and tandem piers are 0.15 and 0.11, respectively. It can be seen that, for a single pier case, at each level, the velocity power spectra are distinguished. Whereas for tandem piers, the maximum strengths are distributed among the piers and resulted in lower peaks. The study concluded that a significant decrease of wake vortices between tandem piers might lead to the occurrence of minimum scour around the tandem rear pier.

Keywords Tandem arrangement · Wake vortices · Velocity power spectra · Strouhal number

L. N. Pasupuleti (✉)

Department of Civil Engineering, Aditya Engineering College, Surampalem, India
e-mail: laxmiraagini@gmail.com

P. V. Timbadiya · P. L. Patel

Department of Civil Engineering, Sardar Vallabhbhai National Institute of Technology, Surat, India
e-mail: pvtimbadiya@ced.ac.in

P. L. Patel

e-mail: plpatel@ced.ac.in

1 Introduction

For safe design of the bridge pier, it is necessary to understand the mechanism of horseshoe vortex and wake vortices which are prime responsible for formation of local scour around the pier. The understanding of such vortices formed around the piers, around closely spaced bridge piers will be different from single pier [1], wherein, the turbulence behind the front piers of parallel pier arrangements is different from turbulence behind single pier under identical flow conditions. Moreover, the studies on flow characterization around the piers, particularly, piers arranged in tandem and staggered configuration is one of the active topics in coastal engineering. In past, few studies were focused on turbulence characterization around tandem piers. Wherein [2] found, turbulence kinetic energy, turbulence intensities and Reynolds shear stresses were decreased behind the front pier in tandem arrangement ($S/d = 3$, where, S was the center-to-center spacing, d is diameter of the pier) in comparison to single pier using Acoustic Doppler Velocimeter (ADV) on rigid beds. The effect of skew angles ($\theta = 0^\circ, 30^\circ, 45^\circ, 60^\circ, 90^\circ$) on local scour with respect to flow direction around tandem piers ($S/d = 2$) was investigated by [3, 4]. They found, at 45° , the maximum scour depths occurred at both the piers and suggested 30° is the best alignment for rear pier position in tandem configuration. Keshavarzi et al. [5] explored Reynolds shear stresses, turbulence intensities, and turbulence kinetic energy and around tandem piers ($S/d = 2.5$) using Particle Image Velocimeter (PIV). They found, large turbulence was produced behind the front pier vis-à-vis single pier. Vijayasree et al. [6] explored flow characterization around single, tandem, and oblong piers using ADV. They concluded, turbulence kinetic energy, Reynolds shear stress, and turbulence intensities are significantly decreased behind the oblong pier vis-à-vis tandem front and isolated pier. Few studies [7–15] were focused on turbulence fields around the single pier and identified strong turbulence behind the pier.

Extensive experimentations were undertaken on scour around single pier to estimate the scour depth. The studies focused on turbulence fields around the closely spaced tandem piers and shown the best alignments of rear pier position. However, the vortices formed around the tandem piers, particularly in the wake regions of both front and rear piers are scarce in the literature. The limited availability of studies on quantification of wake vortices around tandem piers, motivated the authors to carry the present study. The objective of the present study is to quantify the strengths of wake vortices shed from the pier boundary through velocity power spectra at 5, 30, and 50% for a given flow depth in both front and rear pier of tandem arrangement, and compared the same with single pier under identical flows.

2 Materials and Methods

2.1 Experimental Set-Up

A recirculation sediment transport flume (15 m long, 0.89 m wide, and 0.6 m height) was used to carry out the experiments, situated at Advance Hydraulics Laboratory in the department of Civil Engineering, Sardar Vallabhbhai National Institute of Technology, Surat, Gujarat, India, plan and elevation of flume is shown in Fig. 1 [16]. A 8.0 m long glass sided walls were fixed for clear view of flow. To allow the smooth flow over the working section of 6 m, 2 honey comb cages separated by 1.0 m are placed at the inlet. The flow depth over the working section will be maintained by tail gate, which is situated at the outlet of the flume. The steady uniform flow over the working section will be maintained through SCADA system.

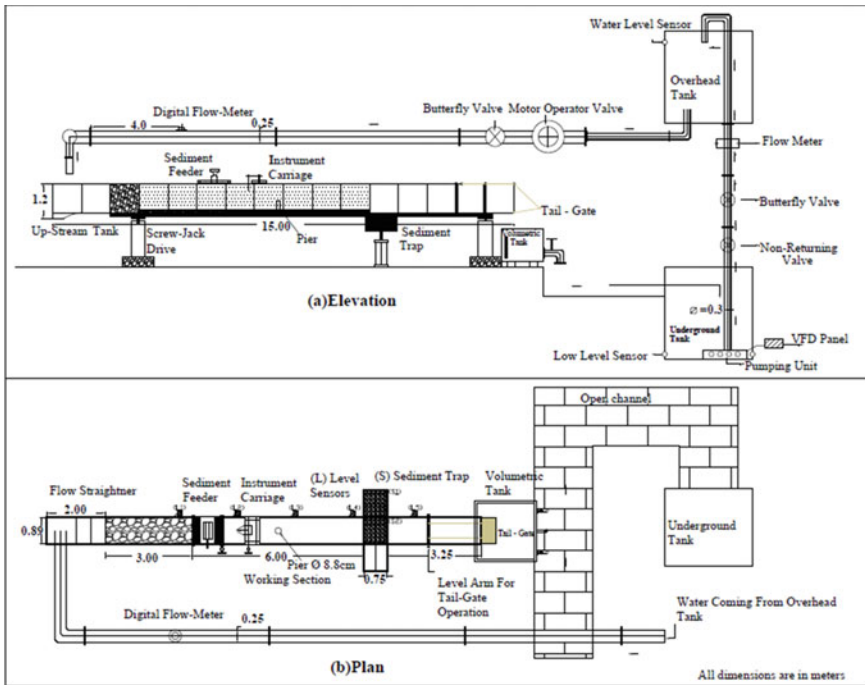


Fig. 1 Schematic of experimental set-up a elevation, b plan

Table 1 Flow conditions used in the experimentation

Discharge (m ³ /s)	Flow depth (Z ₀) (m)	Flow Reynolds No., Re (10 ⁴)	Mean approaching flow velocity (U) (m/s)	Diameter of pier (m) (d)	Longitudinal slope (10 ⁻⁴)
0.022	0.105	2.47	0.235	0.088	3.8

2.2 Instrumentation and Data Collection

In current study, experiments were performed over the rigid bed, wherein a single pier ($d = 8.8$ cm) was glued over the channel bottom, positioned at 8.0 m from the inlet. The flow conditions (see Table 1) were maintained constant during all the experiments. The instantaneous 3D velocity measurements, undertaken using 16 MHz micro down looking Acoustic Doppler Velocimeter (ADV) was used to collect three-dimensional velocities around the pier at different grids (see Fig. 2). Here, u, v, w in X, Y, Z directions are expressed as $u = \bar{u} + u', v = \bar{v} + v', w = \bar{w} + w'$, where $\bar{u}, \bar{v}, \bar{w}$ are time-averaged velocities, and u', v', w' are fluctuating components in X, Y, Z directions. Here, X is longitudinal, Y is transverse, and Z is vertical flow direction. After the collection of data around single pier, the pumps were stopped and flume was allowed to drain. The rear pier was positioned at $S/d = 2$, here, S , center-to-center spacing, and collected the three-dimensional velocity data around front and rear piers under identical flow conditions (Fig. 3b). The collected raw data were processed to remove the noise, and velocity signals were de-spiked using a phase space threshold de-spiking technique (Fig. 4). Similar technique was adopted in the previous studies [17–19] for de-spiking the velocities. The detrended de-spiked signals need to check on Kolmogorov's scale for successful capturing of inertial subrange. The three-dimensional velocity profile plotted on Z/Z_0 vs U^+, V^+, W^+ , (see Fig. 5). Here, $U^+ = \bar{u}/U, V^+ = \frac{\bar{v}}{U}$, and $W^+ = \bar{w}/U$. From Fig. 5, it depicts, measured velocity profile U^+ at 1.0 m distance from the upstream pier follows the log law up to flow depth of 5.5 cm from the channel bottom. On other hand, the variation of V^+ and W^+ are nearer to zero. This can be ascertained that flow was developed in the working section.

3 Results and Discussion

In current study, the power spectra analysis was carried to quantify the wake vortices defused from pier boundary in single and tandem piers, shown in Fig. 6 and Fig. 7, respectively. Here, the velocity power spectra were computed at different levels, 5% ($Z = 0.525$ cm), 30% ($Z = 3.15$ cm), and 50% ($Z = 5.25$ cm) of flow depth using detrended velocity signals with the help of the Fast Fourier Transform (FFT) packages available in the Origin-2019b. Here, the computed spectra was multiplied

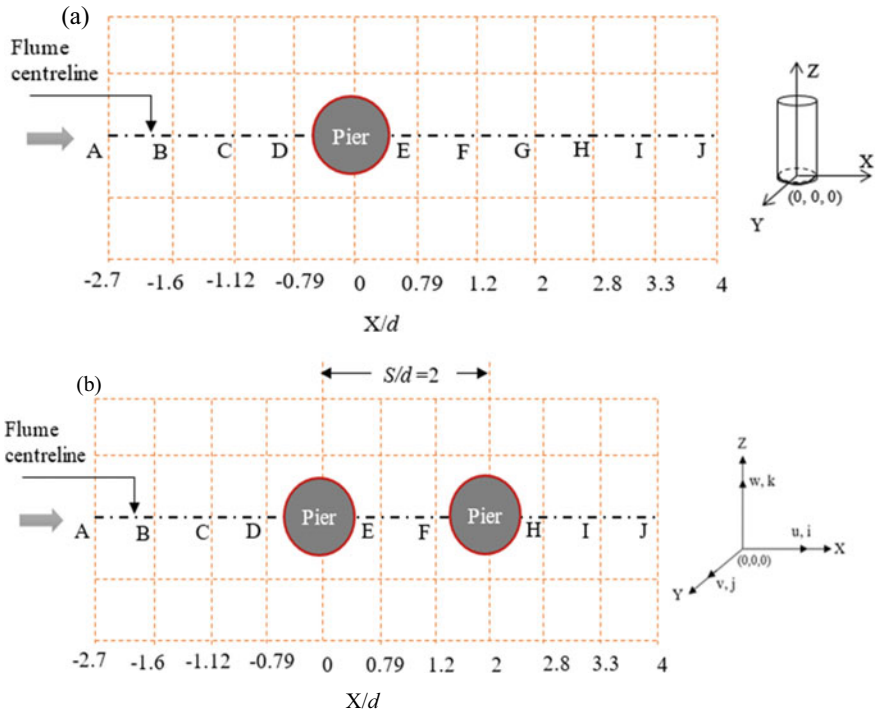


Fig. 2 Schematic of ADV data collection for a single pier and b tandem piers

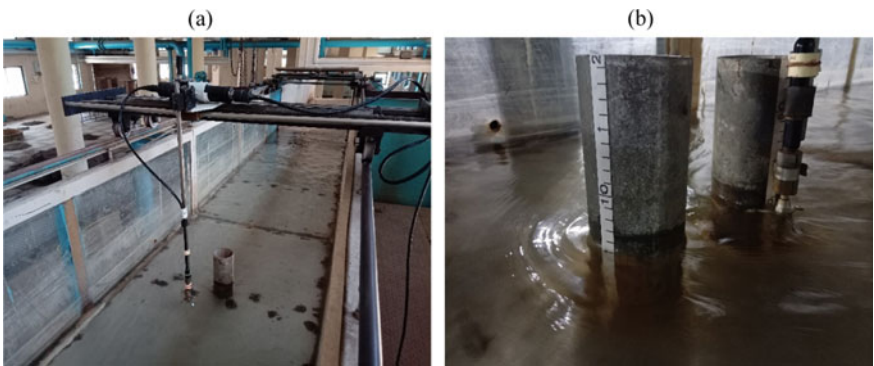


Fig. 3 Photographs of ADV data collection for a single pier and b tandem piers

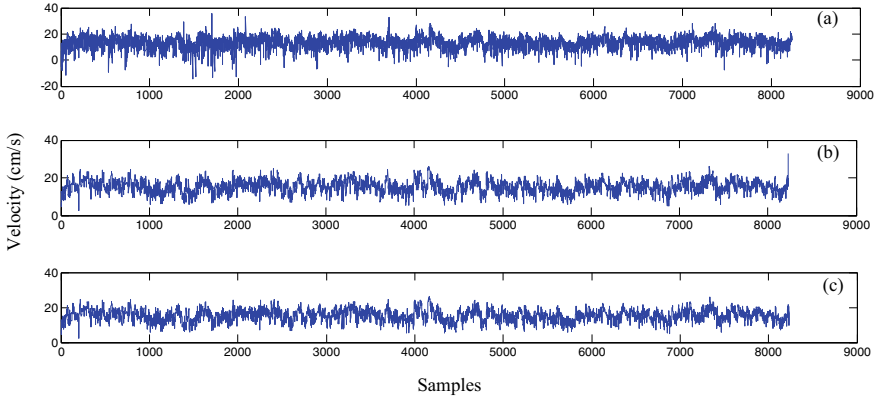


Fig. 4 **a** Sample time series of velocity measurement **b** cubic interpolated time series after removal of noise contamination **c** de-spiked and cubic interpolate time series

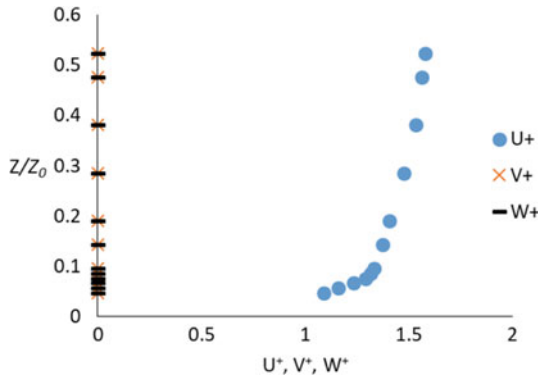


Fig. 5 Velocity distribution over rigid bed at 1 m upstream of single pier

with corresponding frequency [$f.P_u(f)$, $f.P_v(f)$, and $f.P_w(f)$ (cm^2/s^2)] to present the spectra in variance preserve form for streamwise, transverse, and vertical velocity components, respectively. To quantify the strength of wake vortices behind the piers of single and tandem arrangements, the Strouhal number (St) is computed using $St = fd/U$, where f is the dominant vortex shedding frequency, d is the diameter of pier, U is the approaching mean flow velocity [2, 17, 19]. From Figs. 6 and 7, it can be seen that the dominant component is transversal velocity component ($f.P_v(f)$) in the wake regions of single and tandem piers (for locations, refer, Fig. 2). Whereas other two velocity components (streamwise and vertical) are shown weak strengths at corresponding locations.

The velocity power spectra reveals, the strength of wake vortices is significantly decreased at front tandem pier vis-à-vis single pier. It is observed that the transversal component is 2.5 times higher for single pier as compared to front tandem pier.

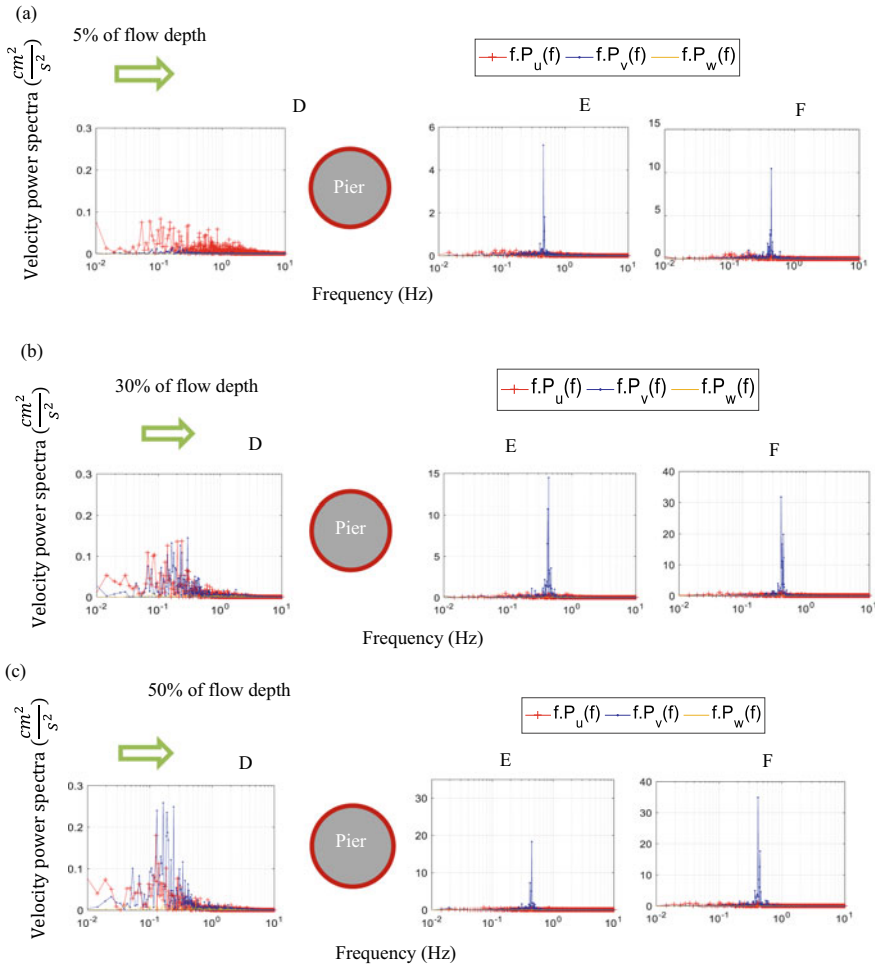


Fig. 6 Velocity power spectra at flow depths **a** 5%, **b** 30%, and **c** 50%, at flume centerline around the single pier

Further, these strengths are increased with level while moving away from the bed. The maximum strengths are seen at 50% ($Z = 5.25$ cm) and minimum are observed at 5% ($Z = 0.525$ cm) for single and tandem piers. Further, the Strouhal number reveals, the large size eddies are formed behind the single pier with $St = 0.15$ as compared to front tandem pier ($St = 0.11$). It can be seen; the size of eddy is increased by 35% behind the single pier vis-à-vis front tandem pier. The eddies of small size cause high-frequency fluctuations, whereas larger eddies cause small-frequency fluctuations [20]. The high frequency of all three components of velocity fluctuation in downstream of the front pier in single and tandem arrangements indicated the presence of smaller eddies in the region. It is to be noted that large size of the eddy is governed by the size of the

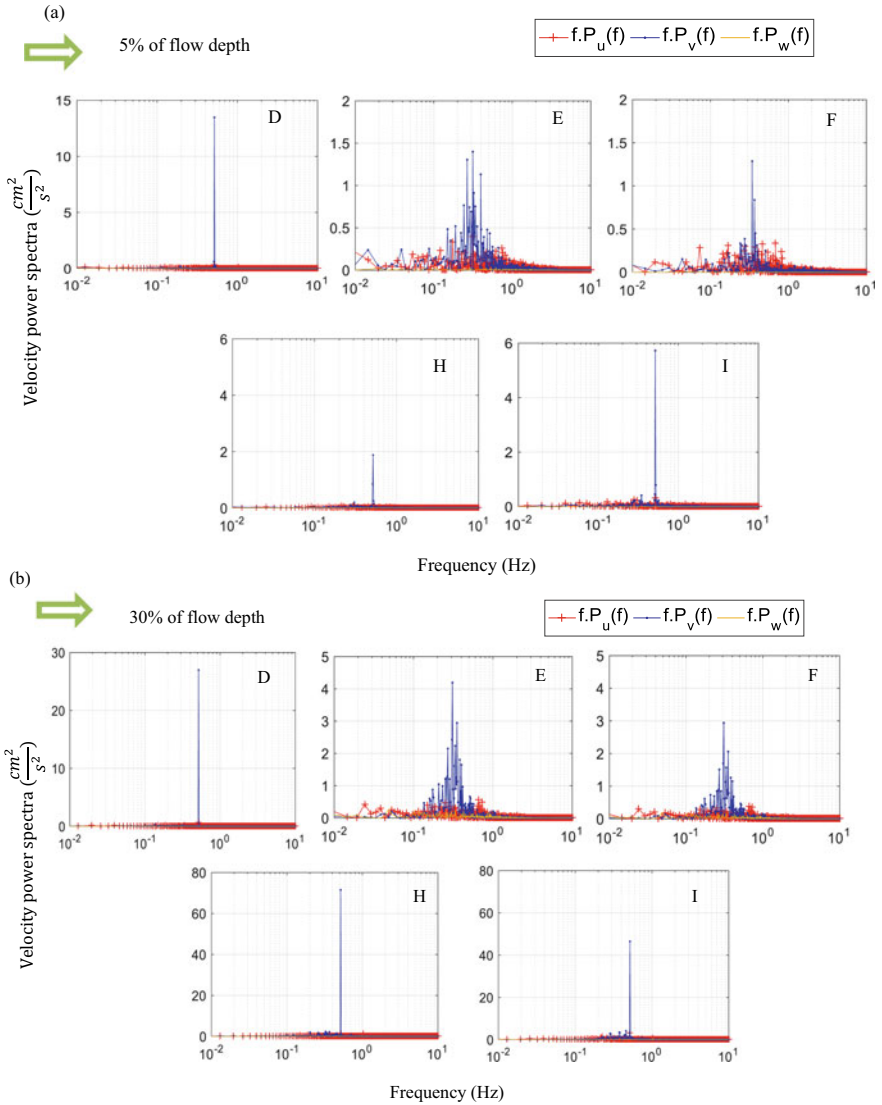


Fig. 7 Velocity power spectra at flow depths **a** 5%, **b** 30%, and **c** 50%, at flume centerline around the tandem pier

flow depth itself, whereas the smallest size of the eddy is determined by viscosity, and it decreases with an increase in average velocity of flow [21]. The comparisons of spectra in the front pier and rear pier of tandem arrangement depicted, the strengths are increased significantly as compared to the front pier, as and when the fluid particles reached to rear pier. Due to the significant decrease in strength of wake vortices between tandem piers, results to have a minimum scour around the tandem rear pier.

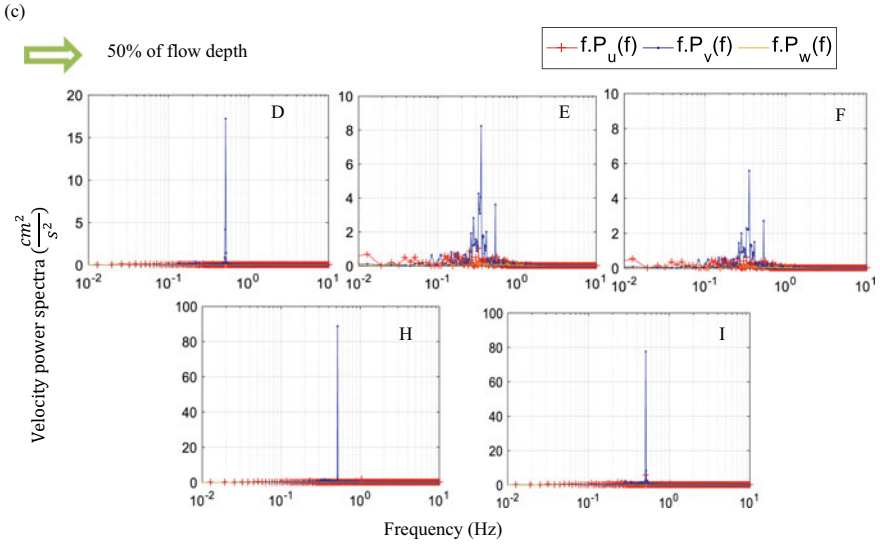


Fig. 7 (continued)

4 Conclusions

The following conclusions are drawn from the current study:

- The wake vortex strength has been found 2.5 times higher in single pier than front tandem pier. These strengths are increased with level and found maximum at 50% ($Z/Z_0 = 0.5$) in single and tandem piers.
- Transversal velocity component is dominant one, and other two velocity components (streamwise and vertical) are shown weak spectra in the wake regions of single, front, and rear piers of tandem arrangement.
- The Strouhal number, St is 0.15 and 0.11 for single and front tandem pier, respectively. It reveals, the large size eddies are formed behind the single pier vis-à-vis front tandem pier. Due to the significant decrease of wake vortex strength between tandem piers might lead to the occurrence of minimum scour around the tandem rear pier.

Acknowledgements Authors are thankful to the Centre of Excellence (CoE) on “Water Resources and Flood Management” at Sardar Vallabhbhai National Institute of Technology (SVNIT)-Surat, Gujarat, India funded by TEQIP-II, Ministry of Education (MoE), Government of India. The experimental facility utilized in the current work was developed through the Department of Science and Technology, Government of India funded research project on “Erosion of non-uniform unimodal and bimodal sediments” which authors duly acknowledged.

References

1. Zhou K, Duan JG, Bombardelli FA (2020) Experimental and theoretical study of local scour around three-pier group. *J Hydraul Eng* 146(10):04020069
2. Ataie-Ashtiani B, Aslani-Kordkandi A (2013) Flow field around single and tandem piers. *Flow Turbul Combust* 90(3):471–490
3. Memar S, Zounemat-Kermani M, Beheshti A A, De Cesare G, Schleiss AJ (2018) Investigation of local scour around tandem piers for different skew-angles. *E3S Web Conf* 40:03008
4. Hannah CR (1978) Scour at pile groups. Research Report 28–3, University of Canterbury, Christchurch, New Zealand
5. Keshavarzi A, Ball J, Khabbaz H, Shrestha CK, Zahedani MR (2018) Experimental study of flow structure around two in-line bridge piers. *Proc Inst Civ Eng Water Manage* 171(6):311–327
6. Vijayasree BA, Eldho TI, Mazumder BS (2019) Turbulence statistics of flow causing scour around circular and oblong piers. *J Hydraul Res* 57(6):1–14
7. Dargahi B (1989) The turbulent flow field around a circular cylinder. *Exp Fluids* 8:1–12
8. Graf WH, Istiarto I (2002) Flow pattern in the scour hole around a cylinder. *J Hydraul Res* 40(1):13–20
9. Muzzammil M, Gangadhariah T (2003) The mean characteristics of horseshoe vortex at a cylindrical pier. *J Hydraul Res* 41(3):285–297
10. Kirkil G, Constastantinescu G, Ettema R (2008) Coherent structures in the flow field around a circular cylinder with scour hole. *J Hydraul Eng* 134(5):572–587
11. Dey S, Raikar RV (2007) Characteristics of horseshoe vortex in developing scour holes at piers. *J Hydraul Eng* 133(4):399–413
12. Kumar A, Kothiyari UC (2012) Three-dimensional flow characteristics within the scour hole around circular uniform and compound piers. *J Hydraul Eng* 138(5):420–429
13. Ataie-Ashtiani B, Aslani-Kordkandi A (2012) Flow field around side-by-side piers with and without a scour hole. *Europ J Mech Fluids* 36:152–166
14. Graf WH, Yulistiyanto B (1998) Experiments on flow around a cylinder: the velocity and vorticity fields. *J Hydraul Res* 36(4):637–653
15. Gautam P, Eldho TI, Mazumder BS, Behera MR (2019) Experimental study of flow and turbulence characteristics around simple and complex piers using PIV. *Exp Thermal Fluid Sci* 100:193–206
16. Pasupuleti LN, Timbadiya PV, Patel PL (2020) Bed level variations around the submerged tandem piers in sand beds. *ISH J Hydraul Eng* 28(1):149–157
17. Sarkar K, Chakraborty C, Mazumder BS (2016) Variations of bed elevations due to turbulence around submerged cylinder in sand beds. *Environ Fluid Mech* 16(3):659–693
18. Pasupuleti LN, Timbadiya PV, Patel PL (2021a) Vorticity fields around a pier on rigid and mobile bed channels. *ISH J Hydraul Eng* 1–10
19. Pasupuleti LN, Timbadiya PV, Patel PL (2021) Flow field measurements around isolated, staggered, and tandem piers on a rigid bed channel. *Int J Civ Eng* 20:569–586
20. Garde RJ (1994) *Turbulent flow*. New Age International Limited, New Delhi
21. Garde RJ (2005) *River morphology*. New Age International Publishers, New Delhi